Improvement of the mechanical and flame-retardant properties of polyetherimide membranes modified with Graphene oxide

Virginia Lopez [1], A. Paton-Carrero[1], Amaya Romero[1], Jose Luis Valverde[1] and Luz Sanchez-Silva[1]

1 Department of Chemical Engineering, University of Castilla La Mancha, Av. Camilo Jose Cela 12, 13071 Ciudad Real, Spain

Correspondence to: Luz Sanchez-Silva (MariaLuz.Sanchez@uclm.es)

ABSTRACT

Polyetherimide (PEI) membranes doped with different amounts (1-5 wt.%) of Graphene Oxide (GO) were prepared through a solution casting method. The effect of the Graphene Oxide incorporation on mechanical and flame-retardant properties was investigated by XDR, FTIR and SEM analyses. Results showed that the addition of 5 wt.% of GO into the membranes caused a 30% of improvement in the tensile strength and a significant increase in the glass transition temperature. Flame-retardant properties were improved when the amount of Graphene Oxide into PEI membrane was increased. These improvements in the membrane composites expand its application for aerospace and building industries.

1. Introduction

In 2004 Novoselov *et al.* discovered a simple method to isolate a mono-atomic layer of sp^2 carbon, the so-called graphene, in which a single layer of carbon atoms is densely packed into a benzene-ring structure [1]. Graphene is the ideal sp^2 carbon-based material and, thank to its exceptional properties, hundreds of articles about graphene functionalization and multitude of polymer/graphene composite materials with different properties and applications have been reported in literature [2,3]. For that reason, graphene is considered as the starting point for developing other sp^2 carbon nanostructures [4].

Ideal graphene (monolayer Graphene) exhibits exceptional mechanical, optical, electronic and thermal properties. However, non-ideal Graphene (Few-Layer Graphene, FLG), which can be massively produced, is typically used in composite elaboration, although the physic-chemical properties of this type of graphene are worse than those of ideal graphene [5].

Polyetherimide (PEI) is a kind of high-performance polymer, which possesses a high glass transition temperature ($T_g \approx 215$ ºC), excellent flame retardant properties, low smoke

generation, good mechanical properties, dielectric strength, chemical stability, multiple solvent resistance, high heat resistance and good film-forming properties [6-8]. This polymeric material is usually synthesized to produce reusable medical devices, analytical and electrical instrumentation for flexible printed circuit boards [9] and, electronic insulators [10].

Polymer nanocomposites usually consists of a polymeric matrix together with different high-surface-area reinforcing fillers including carbon nanotubes, carbon nanofibers, nanoclays, carbon black, graphene platelets, and so on [11].

There are different published works of PEI composites. Wu *et al.* reported improvements in the tensile strength, modulus and, thermal and electrical stability in AIN (aluminum nitride)/PEI composites [12]. Huang *et al.* studied the morphology, solvent resistance and thermal properties of polyetherimide/montmorillonite nanocomposites prepared by melt intercalation. PEI/MMT nanocomposites exhibited a substantial increase of both the glass transition temperature and thermal decomposition temperature and, a dramatic decrease in the solvent uptake if compared to that of the neat PEI [7]. Peijiang et al. evaluated the mechanical, thermal and dielectric properties of GO as nanofiller, showing that ultrasonication provides an uniform dispersion of the GO into the matrix that results in an improvement of the tensile strength, flexural strength, impact strength just with the addition of 1 wt.% GO. Besides, GO addition increased the glass transition temperature and enhanced the thermal stability and the dielectric constant compared with the pure material[13]. Cakar *et al.* developed PEI/graphite composites films that can be used as a sensor element to detect chloroform and chlorobenzene [14]. Hwang *et al*. studied the thermal and mechanical properties of PEI/functionalized graphene oxide composites. Either, alkylaminated (enGO) and phenyl-aminated (pnGO) graphene oxides were used and, a solution casting method to prepare PEI/GO composites with 1, 2 and 3 wt.% filler contents. The elastic modulus and glass transition temperature (Tg) of the three types of GO/PEI composites were higher than those from the neat PEI [15].

In this work, it has been investigated the preparation of PEI/GO membranes using a solution casting method. The influence of the addition of different GO amounts on the mechanical and thermal properties was evaluated in detail.

2. Experimental

2.1. Materials

Polyetherimide (PEI) was purchased from General Electric Plastics. Chloroform solvent was purchased from Sigma Aldrich. Graphite powder (< 20 μm) was supplied by ALDRICH CHEMISTRY. Potassium permanganate ($KMnO_4$), sulfuric acid (H_2SO_4), chlorhydric acid (HCl), hydrogen peroxide (H_2O_2) and ethanol (CH_3CH_2OH) were supplied by PANREAC. Monohydrate hydrazine with a purity grade of 98% was supplied by SIGMA-ALDRICH and ascorbic acid with a purity grade of 99% was supplied by VWR.

2.2. Graphite Oxide preparation.

Graphite Oxide was first synthesized by the *Improved Hummers Method* [16]. In this method, $KMnO_4$ was used as the oxidizing agent. A mixture of 15 grams of graphite and 45 grams of $KMnO_4$ (1:3) was slowly added to 400 ml of H_2SO_4 under constant agitation to avoid any explosion. The mixture was maintained at 50ºC for 3 hours. Then, to quench the reaction, the mixture was added into a beaker, containing a mixture of 400 g of flake ice and 3 ml of H_2O_2. The mixture was filtered under vacuum and, finally, it was washed with 200 ml of deionized water, HCl and CH_3CH_2OH. To conclude, the compact cake was dried at 100ºC overnight.

2.3. PEI/GO membranes fabrication

Figure 1 shows a schematic illustration of the experimental synthesis procedure steps of PEI/GO membranes using a casting method. Appropriate volume of chloroform was added to the beaker containing Graphite Oxide. Subsequently, this mixture was sonicated for 1 hour using an amplitude of 50% and a full cycle. With the sonication process, Graphite Oxide turns into Graphene Oxide. After that, certain amounts of Graphene Oxide and PEI were stirred for 2 hours. Finally, the solutions were casting onto a clean glass plate with a cover for 48 hours to delay solvent evaporation from the nascent membrane. The membrane obtained were 7 cm of diameter and 0.2 mm thickness. The recipe conditions used in the preparation of all samples are specified in Table 1. Notation for all samples are also given in Table 1.

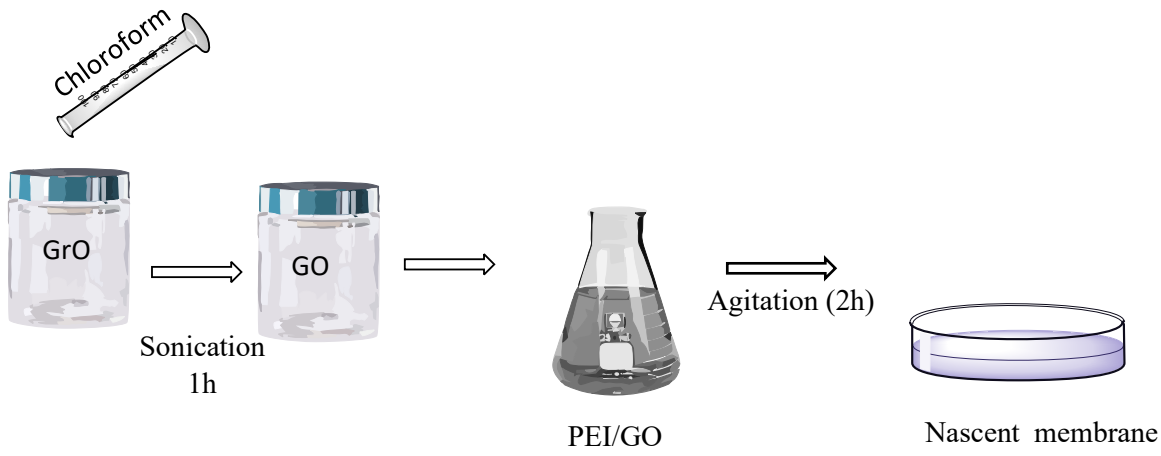

Figure 1. Schematic illustration of the experimental synthesis process of PEI/GO membranes.

Table 1. Solvent and reagents used in the preparation of neat PEI and PEI/GO membranes.

Membranes	GrO (mg)	PEI (mg)	Chloroform (ml)
Neat PEI	0	800	18
PEI/1wt.%GO	8	792	18
PEI/2wt.%GO	16	784	18
PEI/3wt.%GO	24	776	18
PEI/4wt.%GO	32	768	18
PEI/5wt.%GO	40	760	18

2.4 . Characterization

X-Ray Diffraction (XRD): X-Ray diffraction was performed in a PHILIPS, PW-1711 model diffractometer with CuKα radiation (λ = 1,5404). The samples were scanned at a rate of 0.02º $step^{-1}$ over the range 5º ≤ 2θ ≤ 90º (scan time = 2s $step^{-1}$) and the diffractograms were compared with the PDF-ICDD references. Different parameters can be obtained from XRD. Interlaminar space can be calculated using Bragg equation (d_{002}) [17]. The packing size of Graphene planes can be calculated by the Debye-Scherrer equation (Lc) [18].

Infrared Analysis: Chemical interactions between the polyetherimide and the nanomaterial, and the changes induced in the polyetherimide matrix after nanomaterial

incorporation were studied using an infrared spectrometer "Spectrum two" (Perkin Elmer) in the range of 500-4000 cm^{-1}.

Scanning Electron Microscopy (SEM): The morphological structure and pore distribution of the membranes were analysed using a Phenom-ProX scanning electron microscope (Phenom World).

Thermogravimetric analysis (TGA): To study the thermal stability of the synthesized membranes, TGA analysis were carried out using a thermogravimetric analyser (Mettler Toledo TGA/DSC 1 STARe System) at a heating rate of 10 ºC/min. Combustion was carried out under an air atmosphere using a gas flow of 100 NmL/min in the temperature range (0-800 ºC).

Differential scanning calorimetry (DSC): A DSC equipment (2 STARe System) supplied by METTLER TOLEDO was used to determine the glass transition temperature (Tg). Measurements were carried out varying the temperature between 20-200 °C with a heating rate of 10ºC/min in nitrogen atmosphere.

Mechanical properties: A Shimadzu equipment was used to test the tensile stress (Modulus and Elongation) at break of the membranes. Five replicates (16 mm length, by 1.6 mm width) with a gauge thickness of 0.2 mm were used for the analysis. The samples were analysed at a cross-head speed of 1 mm/min. The average values were reported.

Flame retardant properties: these properties were evaluated by measuring the combustion velocity within 10 s. First, adequate membranes (50 mm length x 12 mm x width x 0.2 mm thickness) were prepared. Five replicates were considered; the average values were also reported. The consume velocity (g/s) was calculated by the ratio of the lost weight and the combustion time.

3. Results and Discussion

3.1. GO characterization

After the oxidation of graphite to obtain graphite oxide, 45% of the oxygen atoms were present in the sample as oxygen functional groups verifying that the oxidation procedure followed was quite efficient in terms of incorporation of oxygen groups in the graphite structure. These oxygen functional groups introduced into the material structure [19] were identified by FT-IR to be mainly hydroxyl (O-H), carbonyl (C=O), epoxy (C-O-C) and alcoxy (C-O) groups. The thermal decomposition of the oxygen functional groups present in GO was evaluated by TG analysis (not shown). Obtained results demonstrated that the more labile oxygen groups (hydroxyl and carbonyl ones) were decomposed at

temperatures below 475-500°C whereas the more stable oxygen groups (mainly carboxyl and epoxy ones) were decomposed above 475-500 ºC. It was determined by Raman spectroscopy that I_D/I_G (the intensity of D band relative to the G band) ratio clearly increased if compared to that of the original graphite indicating that structural defects were introduced in the GO as consequence of the attachment of functional groups, such as hydroxyl or epoxy, on the carbon skeleton. Finally, it was demonstrated by XRD analysis that as consequence of the complete oxidation of graphite, e.g. incorporation of different intercalated oxygen functional groups such as hydroxyl, epoxy, carbonyl and carboxyl groups, the interlayer spacing of GO was 2.6 times larger than the original graphite. On the contrary, the crystallite height (Lc) decreased after oxidation from 37 nm in graphite to 5.6 nm in GO [19]. Table 2 shows the most significant XRD and RAMAN parameters of the GO nanofiller.

Table 2. XRD and RAMAN characterization parameters of graphite and GO.

Materials	**Lc**	**d_{002}**	**I_D/I_G**
Graphite	37.10	0.34	0.11
Graphene oxide (GO)	5.62	0.89	0.90

Lc: crystallite height

d_{002}: interlaminar space

I_D/I_G: the intensity of D band relative to the G band

3.2. Morphology and structure of PEI/GO membranes

The composite morphology is a highly critical factor because it impacts on the final composite properties. Figure 2 shows cross-sectional SEM images of neat PEI and PEI/GO (1-5 wt.%) membranes. Figures 2E and 2F (4 and 5 wt.% of GO, respectively) presented agglomerates showing that the agitation time, which remained constant regardless of the amount of nanomaterial added (2 hours), was insufficient, requiring its intensification to suppress the formation of agglomerates.

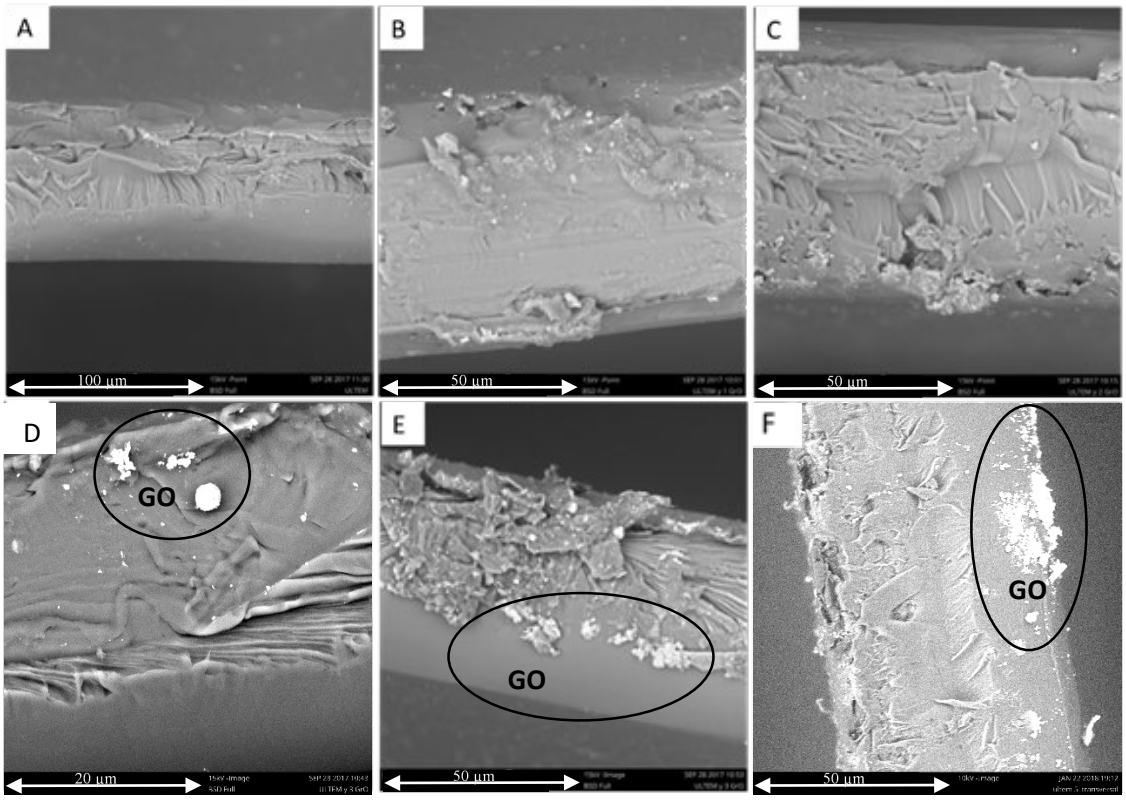

Figure 2. Cross-sectional SEM images of (A) neat PEI, (B) PEI /1wt.% GO, (C) PEI/2wt.% GO; (D) PEI /3wt.% GO; (E) PEI /4wt.% GO; (F) PEI /5 wt.% GO.

Chemical characterization of the neat PEI membrane and PEI/GO membranes (1 and 5 wt.%) was carried out using FT-IR spectroscopy (Figure 3). Peaks at 2970, 2930 and 2875 cm^{-1} correspond to C-H stretching. In addition, FT-IR spectra exhibited characteristic imide absorption peaks (both asymmetrical and symmetrical imide carbonyl stretch) at around 1780 and 1720 cm^{-1}, respectively. Peaks at around 1360 and 747 cm^{-1} were assigned to C-N stretching and bending, respectively, whereas peak at 1240 cm^{-1} was assigned to aromatic C-O-C ether. However, FT-IR GO peaks [19] were not clearly observed in samples PEI/1wt.%GO and PEI/5wt.%GO due to overlap with the characteristic PEI peaks.

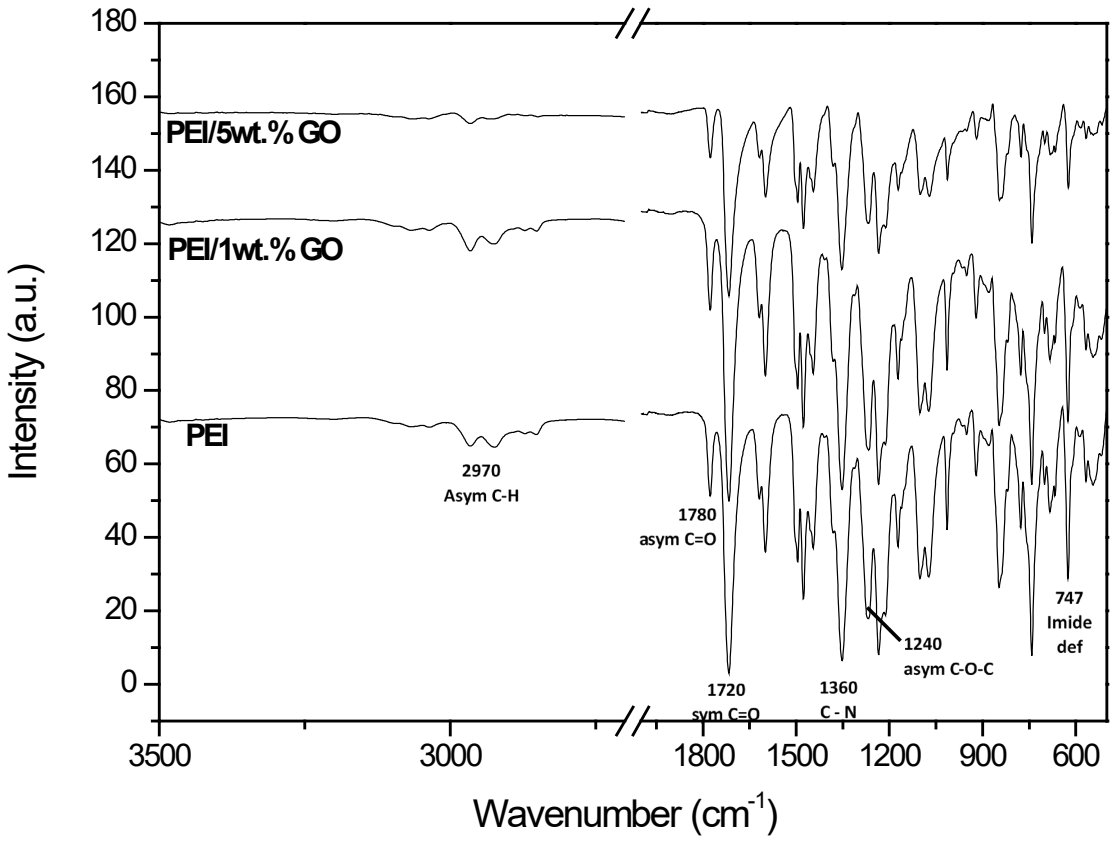

Figure 3. Fourier transform infrared spectroscopy (FT-IR) spectra of neat PEI membrane and PEI/GO membranes (1 and 5 wt.%).

3.3. Thermal analysis of PEI/GO membranes

Thermal decomposition of the PEI/GO membranes was investigated by TGA analysis (Figure 4). Obtained results were compared with those of the neat PEI membrane. TGA curves corresponding to PEI and PEI/GO membranes showed two different weight loss steps. The first step (20-200ºC) was mainly due to the release of residual solvent and water absorbed in the membranes and, to the decomposition of an important part of the functional oxygen groups. A weight loss of 15% was observed in the three PEI membranes indicating that the GO presence did not altered the thermal decomposition of the material. Also, it can be observed that TGA curves were almost similar for neat PEI and PEI/GO membranes until 500ºC, temperature close to the PEI chain decomposition temperature [20]. Finally, although the thermal stability of the three PEI membranes was practically similar, results seem to indicate that thermal stability slightly decreases as the proportion of GO increases.

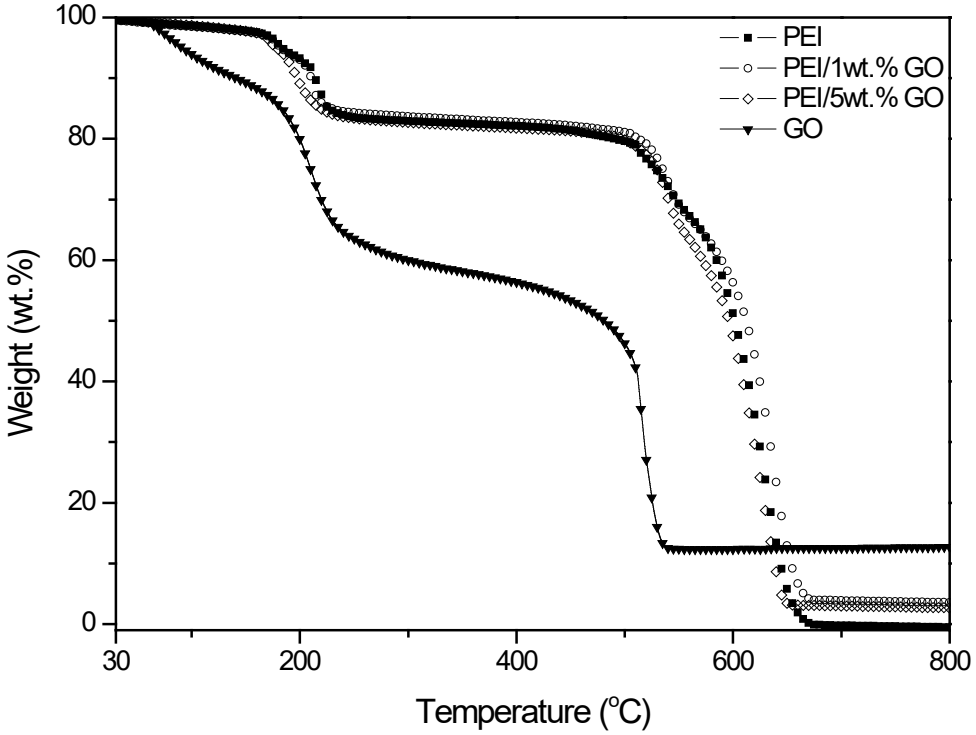

Figure 4. TGA curves corresponding to graphene oxide (GO), PEI and PEI/GO membranes (1 and 5 wt.%).

The glass transition temperature (Tg) of polymers is closely related to the flexibility of the chains. Tg values of the neat PEI and PEI/GO (1-5 wt.%) membranes are listed in Table 3. Tg of the neat PEI was 214 ºC which is in accordance with values reported in literature [21]. Tg values of samples PEI/1wt.%GO and PEI/2wt.%GO were the same as that of the neat PEI membrane. However, glass transition temperature of samples PEI/4wt.%GO and PEI/5wt.%GO membranes increased in 5 °C. The observed Tg increase could be attributed to a strong GO-polymer interaction, which restricts the movement of the polymer chains by the interaction with the -OH groups [15,21].

Table 3. Glass transition temperatures corresponding to the neat PEI and PEI/GO membranes.

Samples	Tg (ºC)
Neat PEI	214
PEI/1wt.%GO	214
PEI/2wt.%GO	214
PEI/3wt.%GO	215
PEI/4wt.%GO	219
PEI/5wt.%GO	219

3.4. Dynamic mechanical analysis.

The incorporation of additives during membrane preparation usually alters the micro-structure of the membranes, and hence their mechanical properties [22,23]. The influence of GO content over the main mechanical properties is observed in Table 4. The tensile strength, modulus and elongation at break were tested with a Shimadzu equipment, using a cross-head speed of 1 mm/min and a high capacity of 10000 N. To assure the reliability of the results, 5 replicates were analyzed, and the average value is showed in the Table 4, together with the experimental error in brackets. We considered neat PEI membrane as reference in order to compare all the membranes composites with it. The tensile strength increased remarkably when 5 wt.% of GO was added, which can be attributed to the improved interaction between the PEI matrix and the GO. GO/PEI membranes showed lower (although similar) modulus than neat PEI. Bor-Kuan *et al*. also showed that there is an optimum amount of additive to reach the higher modulus value [21]. The elongation at break was reasonably decreased with increasing values of GO content due as above-mentioned to the strong interaction between the Graphene oxide and the polymer, which restricts the movement of the polymer chains. These results agree with Tg values.

Table 4. Mechanical properties of the neat PEI and PEI/GO membranes.

Samples	Tensile strength (MPa)	Modulus (GPa)	Elongation at break (%)
neat PEI	43.26 (3.24)	2.43 (0.34)	7.43 (4.87)
PEI/1wt.%GO	23.10 (3.72)	2.10 (0.18)	5.30 (4.76)
PEI/2wt.%GO	33.74 (7.52)	2.40 (0.15)	6.11 (3.73)
PEI/3wt.%GO	43.62 (2.47)	2.27 (0.27)	2.27 (1.49)
PEI/4wt.%GO	41.34 (8.87)	2.25 (0.15)	3.60 (2.24)
PEI/5wt.%GO	52.68 (4.48)	2.40 (0.22)	4.04 (0.47)

3.5. Flame retardant properties.

To assure the reproducibility of the experiment five membranes of 50 mm length x 12 mm x width x 0.2 mm thickness were prepared. The membranes were burned during 10 seconds and the combustion velocity (g/s) was calculated by the difference between the initial and the final weight of the membranes. Neat PEI membrane was considered as a reference and the membranes composites were compared with it. The average values of the five replicates for each study and its errors are shown in the Figure 5. It shows that the combustion velocity (g/s) decreased with increasing values of GO content. These results indicate that the addition of GO can efficiently increase the flame retardancy of PEI membranes, which expands its application field. Thus, the combustion velocity of PEI/5wt.%GO membrane was reduced 15 % with respect of neat PEI membrane.

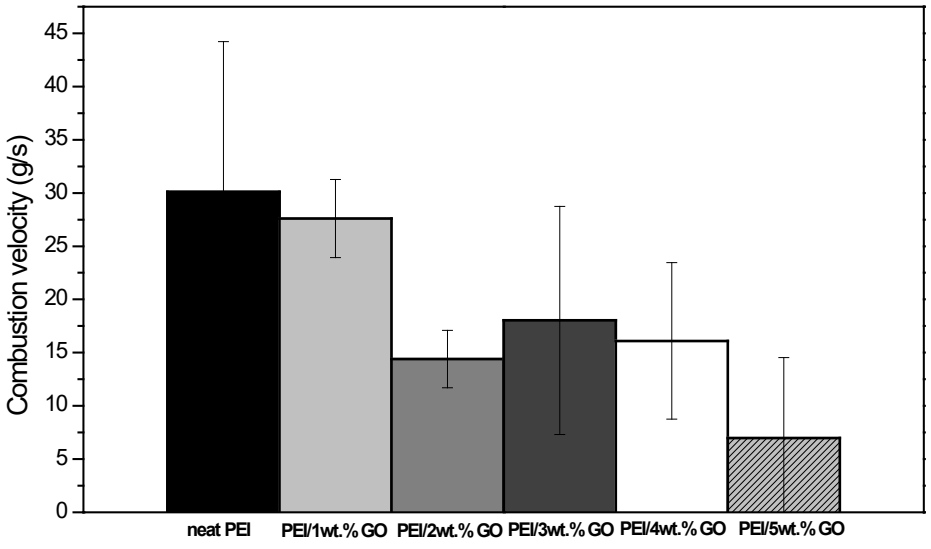

Figure 5. Combustion velocity as a function of the GO content.

4. Conclusions

Composite materials based on PEI/GO membranes were prepared and the effect of adding different amounts of graphene oxide (GO) into the polyetherimide (PEI) matrix was investigated. Results showed that Tg increased with amounts of GO higher than 2 wt.%. Tensile strength showed a 30% of improvement for the PEI/GO 5 wt.% membrane comparing to the neat PEI membrane. The flame-retardant properties were also improved since the velocity of combustion decreased with increasing values of the GO content.

References

1. Novoselov, K. S.; Geim, A. K.; Morozov, S. V.; Jiang, D.; Zhang, Y.; Dubonos, S. V.; Grigorieva, I. V.; Firsov, A. A., Science 306, 666 2004.
2. Radovic, L. R.; Mora-Vilches, C. V.; Salgado-Casanova, A. J. A.; Buljan, A., Carbon 130, 340 2018.
3. Mensah, B.; Gupta, K. C.; Kim, H.; Wang, W.; Jeong, K. U.; Nah, C., Polymer Testing 68, 160 2018.
4. Paillet, M.; Parret, R.; Sauvajol, J. L.; Colomban, P., Journal of Raman Spectroscopy 49, 8 2018.
5. Frank, I. W.; Tanenbaum, D. M.; Van Der Zande, A. M.; McEuen, P. L., Journal of Vacuum Science and Technology B: Microelectronics and Nanometer Structures 25, 2558 2007.
6. Nagendran, A.; Vijayalakshmi, A.; Arockiasamy, D. L.; Shobana, K. H.; Mohan, D., Journal of Hazardous Materials 155, 477 2008.
7. Huang, J. C.; Zhu, Z. K.; Yin, J.; Qian, X. F.; Sun, Y. Y., Polymer 42, 873 2001.
8. Ling, J.; Zhai, W.; Feng, W.; Shen, B.; Zhang, J.; Zheng, W. G., ACS Applied Materials and Interfaces 5, 2677 2013.
9. Yorifuji, D.; Ando, S., Journal of Materials Chemistry 21, 4402 2011.
10. Potts, J. R.; Dreyer, D. R.; Bielawski, C. W.; Ruoff, R. S., Polymer 52, 5 2011.
11. Wu, H.; Drzal, L. T., Journal of Applied Polymer Science 130, 4081 2013.
12. Wu, S. Y.; Huang, Y. L.; Ma, C. C. M.; Yuen, S. M.; Teng, C. C.; Yang, S. Y., Composites Part A: Applied Science and Manufacturing 42, 1573 2011.
13. Liu, P.; Yao, Z.; Zhou, J., High Perform Polym 28, 1033 2016.
14. Cakar, F.; Moroglu, M. R.; Cankurtaran, H.; Karaman, F., Sensors and Actuators, B: Chemical 145, 126 2010.
15. Hwang, Y.; Heo, Y.; Yoo, Y.; Kim, J., Polymers for Advanced Technologies 25, 1155 2014.
16. Lavin-Lopez, M. D. P.; Romero, A.; Garrido, J.; Sanchez-Silva, L.; Valverde, J. L., Industrial and Engineering Chemistry Research 55, 12836 2016.
17. Pope, C. G., Journal of Chemical Education 74, 129 1997.
18. Taylor, A.; Sinclair, H., Proceedings of the Physical Society 57, 126 1945.
19. Romero, A.; Lavin-Lopez, M. P.; Sanchez-Silva, L.; Valverde, J. L.; Paton-Carrero, A., Materials Chemistry and Physics 203, 284 2018.
20. Rajagopalan, M.; Oh, I.-K., ACS nano 5, 2248 2011.
21. Chen, B.-K.; Su, C.-T.; Tseng, M.-C.; Tsay, S.-Y., Polymer Bulletin 57, 671 2006.
22. Ma, Y.; Shi, F.; Wang, Z.; Wu, M.; Ma, J.; Gao, C., Desalination 286, 131 2012.
23. Zafar, M.; Ali, M.; Khan, S. M.; Jamil, T.; Butt, M. T. Z., Desalination 285, 359 2012.